† Electronic Supplementary Material (SI)

Screening of Transition (Y, Zr, Hf, V, Nb, Mo, Ru) and Rare-earth (La, Pr) Elements as Potential Effective Dopants for Thermoelectric GeTe – an Experimental and Theoretical Appraisal

Bhuvanesh Srinivasan,[a,b] Sylvain Le Tonquesse,[b] Alain Gellé,[c] Cédric Bourgès,[a] Leo Monier,[b] Isao Ohkubo,[a] Jean-François Halet,[b,d] David Berthebaud,*[b] Takao Mori*[a]

[a] *WPI International Center for Materials Nanoarchitechtonics (WPI-MANA), National Institute for Materials Science (NIMS), 1-1 Namiki, Tsukuba 305-0044, Japan*

[b] *CNRS-Saint Gobain-NIMS, UMI 3629, Laboratory for Innovative Key Materials and Structures (LINK), National Institute for Materials Science, 1-1 Namiki, Tsukuba 305-0044, Japan*

[c] *Univ. Rennes, CNRS, IPR – UMR 6251, F-35000 Rennes, France*

[d] *Univ. Rennes, CNRS, Institut des Sciences Chimiques de Rennes (ISCR) – UMR 6226, F-35000 Rennes, France*

* **Correspondences**: David.BERTHEBAUD@cnrs.fr (D.B); MORI.Takao@nims.go.jp (T.M)

Table S1. *Le Bail refined structural parameters of doped GeTe samples*

		GeTe	$Ge_{0.995}Zr_{0.005}Te$	$Ge_{0.98}La_{0.02}Te$	$Ge_{0.98}Y_{0.02}Te$	$Ge_{0.98}V_{0.02}Te$	$Ge_{0.995}Hf_{0.005}Te$	$Ge_{0.995}Mo_{0.005}Te$
Hexagonal setting	*a* (Å)	4.1654(1)	4.1654(1)	4.1649(2)	4.1669(2)	4.1672(1)	4.1636(1)	4.1641(2)
	c (Å)	10.6698(3)	10.6613(4)	10.6712(5)	10.6711(6)	10.5725(9)	10.6681(6)	10.6697(5)
	V ($Å^3$)	160.326(3)	160.199(6)	160.31(2)	160.49(9)	159.00(1)	160.16(4)	160.23(9)
Rhombohedral setting	*a* (Å)	4.2933(1)	4.2910(2)	4.2936(3)	4.2942(2)	4.2671(2)	4.2923(2)	4.2929(3)
	α (°)	58.038(1)	58.073(1)	58.027(1)	58.487(1)	53.457(1)	58.026(1)	58.025(1)
	Impurity	Ge	Ge	Ge	Ge	Ge	/	Ge
	a (Å)	5.6558(2)	5.6553(3)	5.6572(5)	5.6565(3)	5.6575(3)	/	5.6557(6)
	R_p	10.9	12.6	17.8	17.2	17.1	13.2	13.1
	R_{wp}	14.5	15.1	20.3	20	21.9	16.3	16.9
	χ^2	2.03	3.11	1.67	2.1	3.31	1.74	2.51

As mentioned in the manuscript, the high values of the agreement factors (R_p, R_{wp}, χ^2) from the fitted patterns are due to the anisotropic peak broadening arising due to the defects in these GeTe compounds.

† Electronic Supplementary Material (SI)

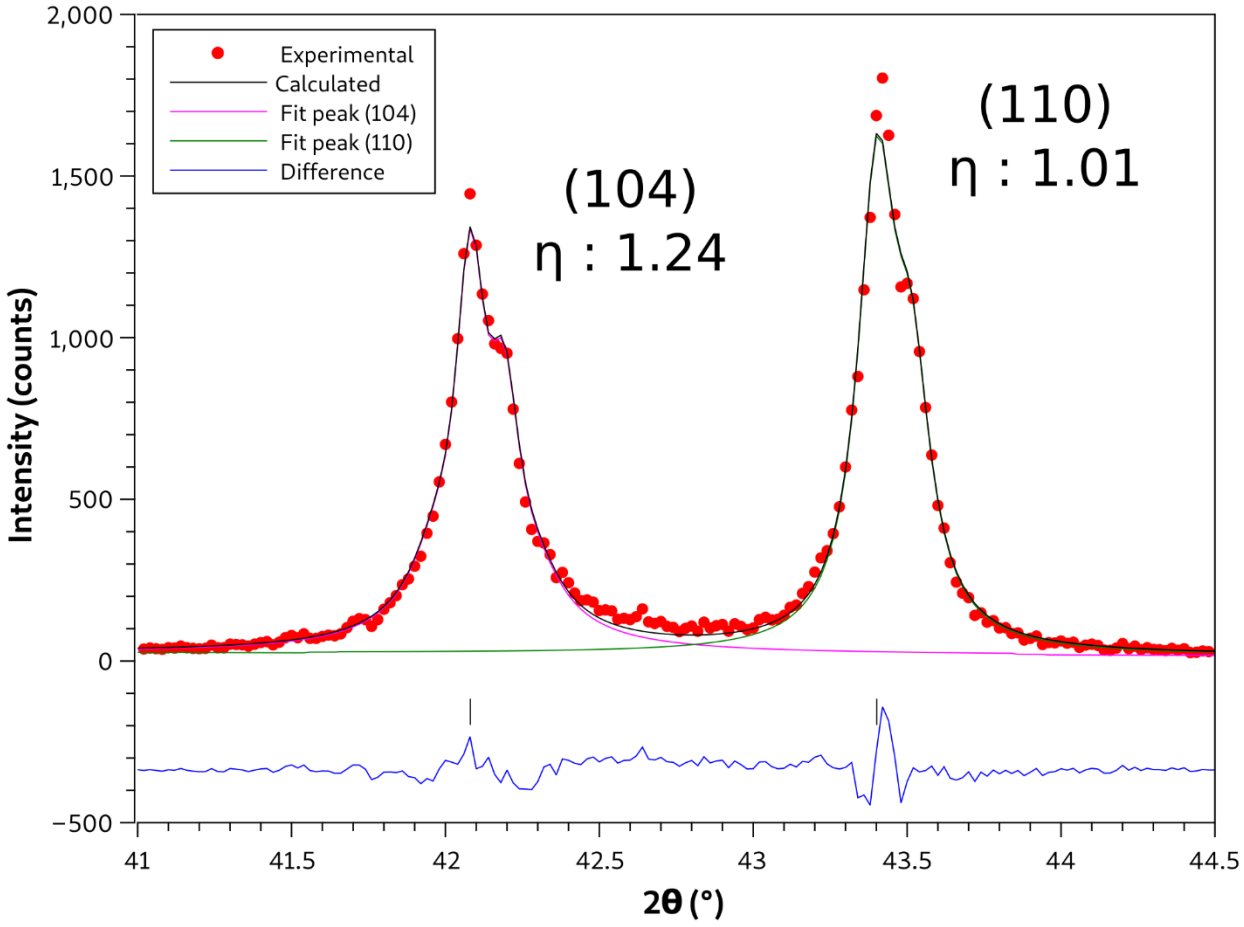

Figure S1. *Experimental and simulated XRD pattern of* $Ge_{0.98}V_{0.02}Te$ *compound showing Bragg peaks with larger tails i.e., more Lorentzian character. Pseudo-Voigt function,* $V_g(x) = \eta\, L(x) + (1-\eta)\, G(x)$, *where* $L(x)$ *and* $G(x)$ *are the Lorentzian and Gaussian functions, while* η *is the refined mixing parameter and it shifts the profile more towards pure Gaussian or pure Lorentzian when approaching 0 or 1 respectively.*

† Electronic Supplementary Material (SI)

Table S2. *Band gap at L-point, and the energy difference between the two valence band maxima from the DFT calculations.*

	Band gap at *L*-point (eV)	**$\Delta E_{L\Sigma}$ (eV)**
$YGe_{63}Te_{64}$	0.254	0.065
$HfGe_{63}Te_{64}$	0.302	0.028
$NbGe_{63}Te_{64}$	0.353	-0.026
$VGe_{63}Te_{64}$	* 0.251	0.065
$MoGe_{63}Te_{64}$	--	0.012
$RuGe_{63}Te_{64}$	--	-0.047

(*) estimated band gap without considering the intruder state

† Electronic Supplementary Material (SI)

Table S3. *Parameters (band gap at L-point, energy difference between the two valence band maxima) extracted from the DFT calculations with different cell sizes for Zr-doped GeTe.*

	Zr %	**Band gap at *L*-point (eV)**	**$\Delta E_{L\Sigma}$ (eV)**
$ZrGe_{31}Te_{32}$	3.13 %	0.386	0.057
$ZrGe_{63}Te_{64}$	1.56 %	0.306	0.024
$ZrGe_{107}Te_{108}$	0.93 %	0.280	0.040
$Ge_{64}Te_{64}$	0.00 %	0.226	0.069
Extrapolation	***0.50 %***	***0.255***	***0.053***

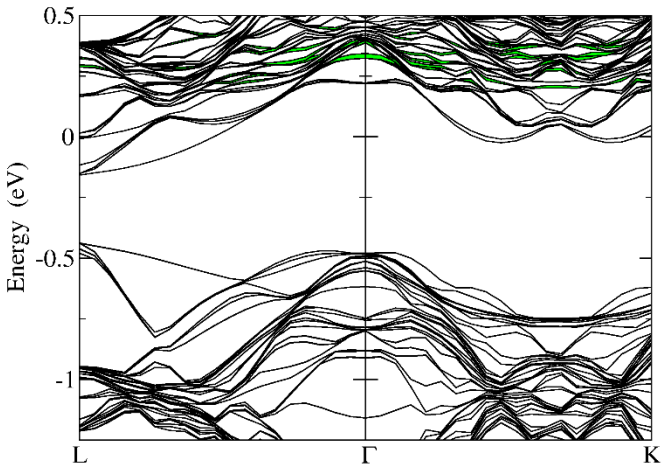

Figure S2. *Band structures of Zr-doped GeTe computed with a larger size of the cell, i.e., for $ZrGe_{107}Te_{108}$ cubic model*

† Electronic Supplementary Material (SI)

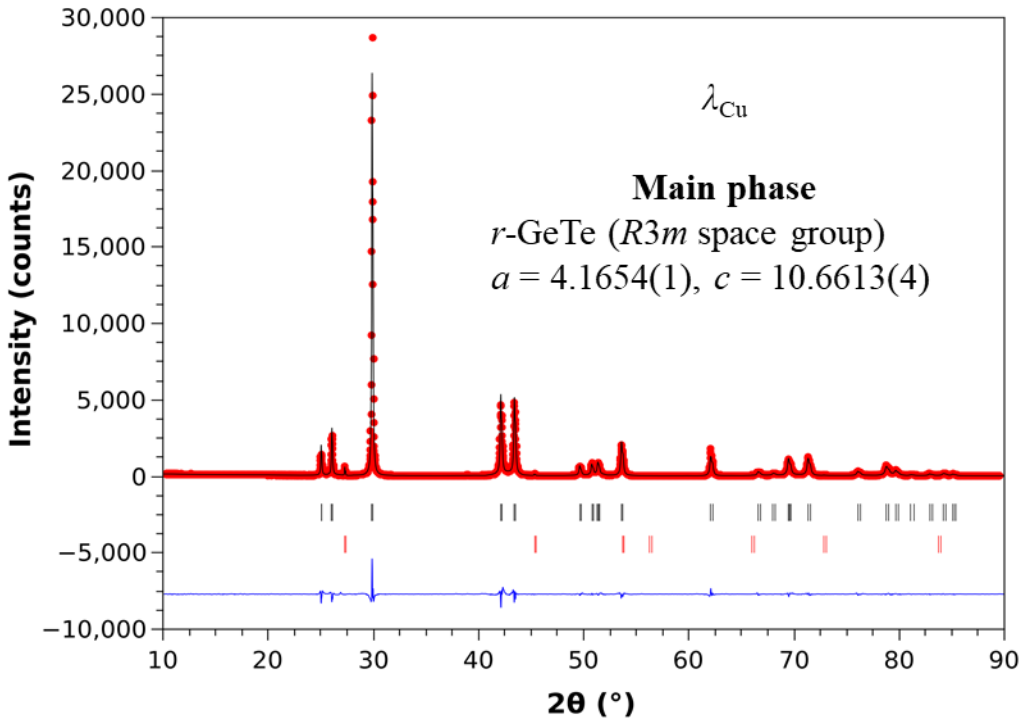

Figure S3. *Le Bail refined room temperature XRD pattern of* $Ge_{0.995}Zr_{0.005}Te$. *The experimental pattern is plotted in red, the calculated pattern in black and the difference in blue. The vertical ticks indicate the Bragg positions of rhombohedral GeTe phase (black) and secondary cubic Ge-phase(red).*

† Electronic Supplementary Material (SI)

***Table S4**. Le Bail refined structural parameters of stochiometric $Ge_{0.995}Zr_{0.005}Te$ and Ge-deficit $Ge_{0.98}Zr_{0.005}Te$*

		$Ge_{0.995}Zr_{0.005}Te$	**$Ge_{0.98}Zr_{0.005}Te$**
Hexagonal setting	*a* (Å)	4.1654(1)	4.1668(1)
	c (Å)	10.6613(4)	10.6613(4)
	V (Å^3)	160.199(6)	160.307(5)
Rhombohedral setting	*a* (Å)	4.2910(2)	4.2914(2)
	α (°)	53.399(1)	58.087(1)
	Impurity	Ge	Ge
	a (Å)	5.6553(3)	5.6577(5)
	% wt.	0.7(2)	0.7(2)
	R_p	12.6	14
	R_{wp}	15.1	17.9
	χ^2	3.11	2.23

† Electronic Supplementary Material (SI)

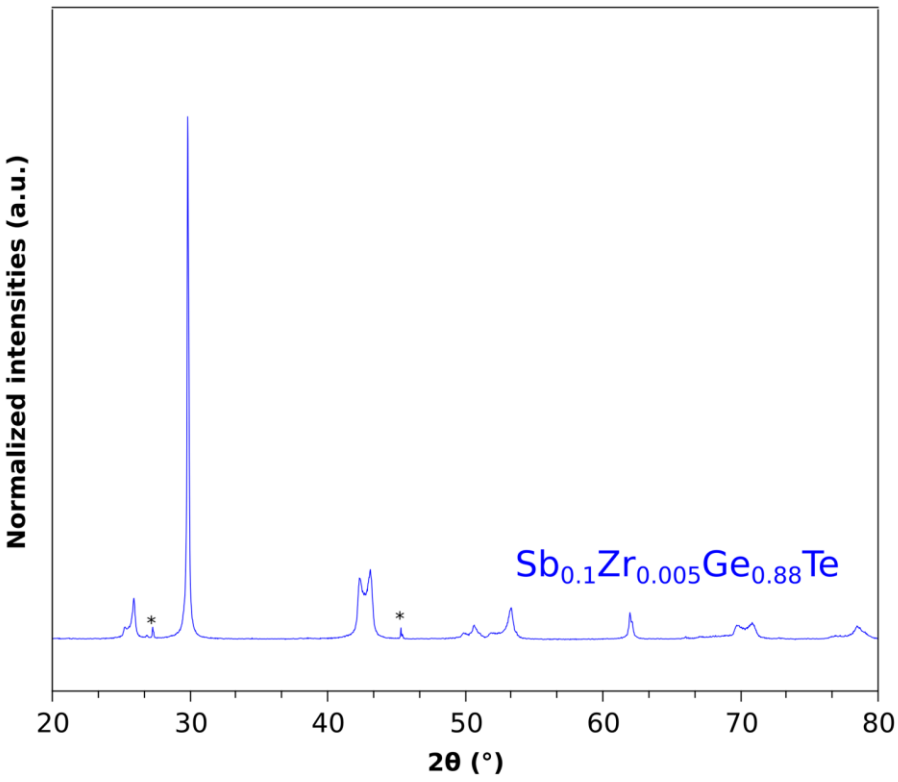

Figure S4. *XRD pattern of $Sb_{0.1}Zr_{0.005}Ge_{0.88}Te$. * denotes secondary cubic Ge-phase (impurity).*

† Electronic Supplementary Material (SI)

Table S5. *Le Bail refined structural parameters of $Ge_{0.895}Zr_{0.005}Sb_{0.1}Te$ and $Ge_{0.88}Zr_{0.005}Sb_{0.1}Te$*

		$Ge_{0.895}Zr_{0.005}Sb_{0.1}Te$	**$Ge_{0.88}Zr_{0.005}Sb_{0.1}Te$**
Hexagonal setting	*a* (Å)	4.1984(4)	4.1997(3)
	c (Å)	10.537(1)	10.530(1)
	V (Å^3)	160.85(3)	160.84(3)
Rhombohe-dral setting	*a* (Å)	4.2675(5)	4.2660(4)
	α (°)	58.931(1)	58.974(1)
	Impurity	Ge	Ge
	a (Å)	5.6553(3)	5.6547(2)
	R_p	23.4	23.9
	R_{wp}	27.3	27.9
	χ^2	10.4	11.6

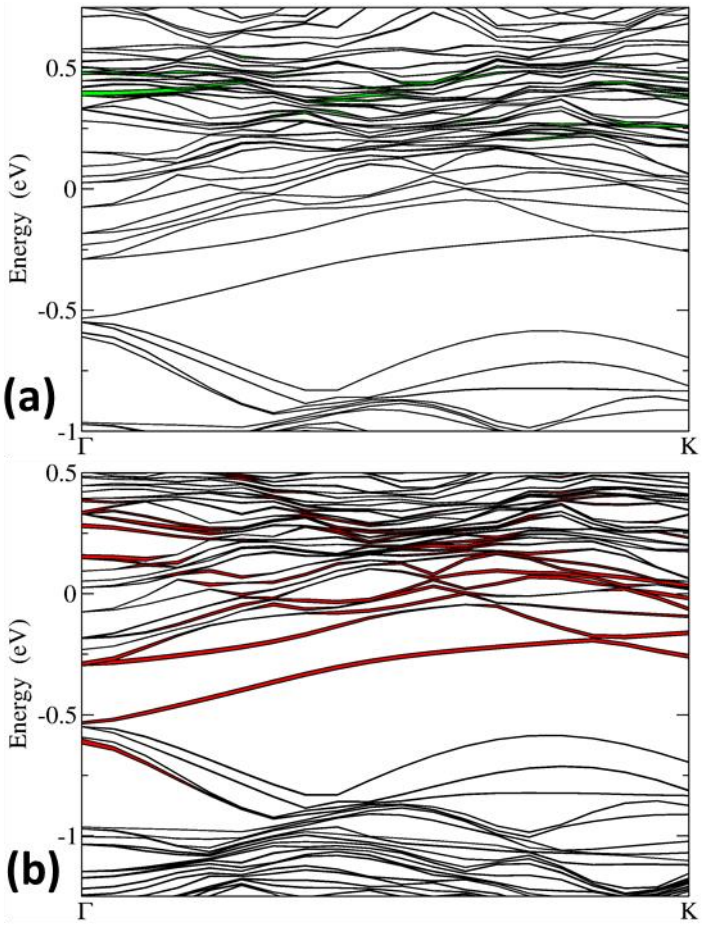

Figure S5. *First-principle calculations on the $Sb_6ZrGe_{67}Te_{64}$ cubic model showing the band structures highlighting (b) Zr projections (in green) and (c) Sb projections (in red). The band structure that was shown in Figure 14 in the main text was computed for an arrangement, where Sb atoms are far away from the center atom, but not all at the same distance. The one that is shown here in SI is computed with an arrangement, where all the Sb atoms are 4^{th} neighbors of the central atom. The differences between the two structures are small and they show consistent results.*